Mps1 regulates spindle morphology through MCRS1 to promote chromosome alignment

Hongdan Yang[a,†], Fengxia Zhang[a,†], Ching-Jung Huang[a], Jun Liao[b], Ying Han[b], Piliang Hao[b], Youjun Chu[b], Xiaoai Lu[a], Wenshu Li[a], Hongtao Yu[c], and Jungseog Kang[a,d,*]
[a]College of Arts and Science, New York University at Shanghai, Shanghai 200122, China; [b]School of Life Science and Technology, Shanghaitech University, Shanghai 201210, China; [c]Howard Hughes Medical Institute, Department of Pharmacology, University of Texas Southwestern Medical Center, Dallas, TX 75390; [d]NYU-ECNU Center for Computational Chemistry, New York University at Shanghai, Shanghai 200062, China

ABSTRACT Accurate partitioning of chromosomes during mitosis is essential for genetic stability and requires the assembly of the dynamic mitotic spindle and proper kinetochore–microtubule attachment. The spindle assembly checkpoint (SAC) monitors the incompleteness and errors in kinetochore–microtubule attachment and delays anaphase. The SAC kinase Mps1 regulates the recruitment of downstream effectors to unattached kinetochores. Mps1 also actively promotes chromosome alignment during metaphase, but the underlying mechanism is not completely understood. Here, we show that Mps1 regulates chromosome alignment through MCRS1, a spindle assembly factor that controls the dynamics of the minus end of kinetochore microtubules. Mps1 binds and phosphorylates MCRS1. This mechanism enables KIF2A localization to the minus end of spindle microtubules. Thus, our study reveals a novel role of Mps1 in regulating the dynamics of the minus end of microtubules and expands the functions of Mps1 in genome maintenance.

INTRODUCTION

Faithful chromosome segregation is highly dependent on the integrity of the mitotic surveillance system, the spindle assembly checkpoint (SAC; Godek *et al.*, 2015; Sacristan and Kops, 2014; Musacchio, 2015). In response to unattached or erroneously attached kinetochores, the SAC is activated and initiates the assembly of the mitotic checkpoint complex (MCC), consisting of BubR1, Bub3, Mad2, and Cdc20, at the kinetochore. The MCC in turn

inhibits the anaphase promoting complex/cyclosome (APC/C) to delay anaphase. This delay provides a time window for the establishment of proper kinetochore–microtubule attachment.

The kinase monopolar spindle 1 (Mps1) plays an important role in initiating and maintaining SAC signaling. It is recruited to unattached kinetochores via the Ndc80 complex and phosphorylates various downstream substrates, including KNL1, Bub1, and Mad1 (Hiruma *et al.*, 2015; Ji *et al.*, 2015; Faesen *et al.*, 2017). Phosphorylation of KNL1 recruits the Bub1–Bub3 complex to the kinetochores for activating the SAC signaling cascade (London *et al.*, 2012; Shepperd *et al.*, 2012; Yamagishi *et al.*, 2012), whereas phosphorylated Bub1 and Mad1 facilitates MCC formation and APC/C inhibition (London and Biggins, 2014; Mora-Santos *et al.*, 2016; Ji *et al.*, 2017).

In addition to its well-established roles in the SAC, Mps1 has been implicated in centrosome duplication, DNA repair, and chromosome alignment (Kasbek *et al.*, 2007; Jelluma *et al.*, 2008; Santaguida *et al.*, 2010; Liu and Winey, 2012; Yu *et al.*, 2016). Several groups have reported that Mps1 actively promotes chromosome alignment during metaphase. Mps1 enhances centromeric Aurora B localization for the correction of erroneous kinetochore–microtubule attachment (van der Waal *et al.*, 2012). In addition, Mps1-dependent phosphorylation of CENP-E relieves the autoinhibition of its motor activity, allowing CENP-E to promote chromosome alignment (Espeut *et al.*, 2008; Lan and Cleveland, 2010). In a recent chemical proteomic study, Ska3 was identified as another

Abbreviation used: ACN, acetonitrile; APC/C, anaphase promoting complex/cyclosome; CFP, cyan fluorescent protein; DIC, differential interference contrast; EGTA, ethylene glycol tetraacetic acid; FHA, forkhead-associated; GAPDH, glyceraldehyde 3-phosphate dehydrogenase; GFP, green fluorescent protein; HCD, high-energy collisional dissociation; HRP, horseradish peroxidase; MAPs, microtubule-associated proteins; MCC, mitotic checkpoint complex; MCRS1, microspherule protein 1; Mps1, monopolar spindle 1; MS, mass spectrometry; RNAi, RNA interference; RT, room temperature; SAC, spindle assembly checkpoint; siRNA, small interfering RNA.

key downstream target of Mps1 for efficient chromosome alignment at metaphase (Maciejowski et al., 2017). Mps1 regulates its own binding to kinetochores. Inactivation of the Mps1 catalytic activity has been shown to stabilize Mps1 binding to kinetochores and hinder normal kinetochore–microtubule attachment (Hewitt et al., 2010; Dou et al., 2015). Thus, Mps1 phosphorylates various downstream targets at kinetochores to achieve efficient chromosome alignment during mitosis.

Microtubule-associated proteins (MAPs) play important roles in chromosome segregation through regulating dynamics of the mitotic spindle. The kinesin-13 family of microtubule motors facilitates microtubule disassembly at the plus and minus ends to coordinate accurate chromosome segregation. In mammals, the three members of this family, KIF2A, KIF2B, and KIF2C/MCAK, play nonoverlapping roles at various mitotic structures, including kinetochores, centrosomes, and the midbody (Manning et al., 2007; Welburn and Cheeseman, 2012). KIF2A first localizes to the mitotic spindle near centrosomes and later moves to the midbody. KIF2C/MCAK, however, localizes to the kinetochore at early mitosis and moves to the centrosome and midbody later. Although all kinesin-13 family members function to destabilize microtubules, double depletion of KIF2A and KIF2C rescues the defect of single KIF2A depletion, suggesting their antagonistic roles (Ganem and Compton, 2004; Rogers et al., 2004). More studies are needed to clarify how different kinesin-13 family members function in mitosis and how they are regulated by mitotic kinases (Jang et al., 2009; Uehara et al., 2013).

The microspherule protein 1 (MCRS1), also known as MSP58, is a MAP that regulates mitotic spindle dynamics. First identified as an interacting partner of the proliferation-related nucleolar protein p120 (Ren et al., 1998), MCRS1 has been implicated in many different biological processes, such as transcriptional regulation, cellular proliferation, senescence induction, and mitotic progression (Lin and Shih, 2002; Okumura et al., 2005; Hirohashi et al., 2006; Andersen et al., 2010; Meunier and Vernos, 2011; Hsu et al., 2012; Fawal et al., 2015; Peng et al., 2015; Lee et al., 2016). During interphase, MCRS1 localizes to the nucleus and nucleolus to regulate gene expression, but it moves to the minus ends of kinetochore microtubules during mitosis to regulate their dynamics (Meunier and Vernos, 2011; Cavazza and Vernos, 2015; Yang et al., 2015). Recent studies have shown that MCRS1 mitotic localization and function are regulated by the KANSL1/3 complex and the Aurora A kinase (Meunier et al., 2015, 2016).

Here, we show that Mps1 interacts with and phosphorylates MCRS1. Phosphorylation of MCRS1 enhances recruitment of KIF2A, a member of the kinesin-13 family, to the minus end of spindle microtubules and facilitates precise chromosome segregation. This finding reveals a novel molecular mechanism of the Mps1 kinase in chromosome alignment and microtubule dynamics to maintain genomic stability.

RESULTS
Mps1 interacts with MCRS1
To further identify downstream targets of Mps1 in chromosome segregation, we carried out a yeast two-hybrid screen using the full-length Mps1 as the bait and identified MCRS1 as an Mps1-interacting protein. MCRS1 had been first known as a transcription regulator localized to the nucleus and nucleolus, but later studies have revealed its mitotic role in regulating microtubule dynamics (Ren et al., 1998; Lin and Shih, 2002; Ivanova et al., 2005; Wu et al., 2009; Meunier and Vernos, 2011).

To further define the interaction domains of two proteins, we constructed several truncations of Mps1 and MCRS1 and examined their interaction by a yeast two-hybrid assay (Figure 1A). When the full-length MCRS1 was tested with the N-terminal, C-terminal, or full-length Mps1, MCRS1 only interacted with the full-length Mps1 (Figure 1B), indicating that neither domain of Mps1 is sufficient for MCRS1 binding. Next, we sought to define the Mps1-binding domain of MCRS1 using the full-length Mps1. Only MCRS1-Δ5, which contains the coiled-coil domain and the FHA domain, interacted with Mps1 (Figure 1B). Interestingly, several serines and threonines in the N-terminal region of Mps1 can undergo autophosphorylation. Thus, the FHA domain of MCRS1 might be binding to Mps1 through these N-terminal phosphoresidues, which are installed by the C-terminal kinase domain. The coiled-coiled domain of MCRS1 may possibly increase the binding valency through mediating the dimerization of the FHA domain.

We further validated the two-hybrid results by an in vitro binding assay with the recombinant full-length Mps1 protein purified from SF9 cells (Figure 1C). The in vitro translated full-length MCRS1 and MCRS1-Δ5 bound to the recombinant Mps1 protein, but not to the recombinant Bub1–Bub3 complex, confirming the Mps1–MCRS1 interaction and the important contributions of the FHA and coiled-coil domains of MCRS1. MCRS1-Δ3 binding was inconclusive due to its nonspecific binding to all baits.

We then asked whether the two proteins interacted in vivo. When endogenous MCRS1 was immunoprecipitated by MCRS1 antibodies from mitotic HeLa cell lysates, it was coprecipitated with endogenous Mps1 (Figure 1D). When MCRS1 truncations were examined for their interaction with Mps1 in mitotic HeLa cells, MCRS1-Δ4 and -Δ5 coprecipitated Mps1, but MCRS1-Δ1 did not. MCRS1-Δ2 and -Δ3 could not be examined because of their instability in cells. (Figure 1E and Supplemental Figure S1A). Interestingly, MCRS1-Δ4 in HeLa cells coprecipitated Mps1, indicating that the middle region of MCRS1 also contributes to Mps1 interaction in HeLa cells. Thus, we concluded that MCRS1 interacts with Mps1 mainly through the middle and C-terminal regions of MCRS1. We also examined whether their binding could be detected in late G2 (Supplemental Figure S1B). Mps1 was efficiently coprecipitated with MCRS1 in G2-arrested cells, suggesting that the interaction of these two proteins was not specific to mitosis.

Mps1 phosphorylates MCRS1
Because Mps1 binds MCRS1, we wanted to examine whether Mps1 phosphorylated MCRS1 in an in vitro kinase assay. In this assay (Figure 2A), Mps1 efficiently phosphorylated MCRS1, but not Nse1, a negative control protein. Furthermore, this phosphorylation was decreased by the presence of the Mps1 inhibitor, reversine, indicating its specificity.

To map the phosphorylation sites of MCRS1, we performed mass spectrometry analysis of MCRS1 in vitro phosphorylated by the Mps1 kinase and identified various serine and threonine sites (Supplemental Table S1). Among them, DEES (27), VESS (65), and EDQT (268) matched the Mps1 phosphorylation consensus sequence, which prefers an acidic amino acid at −2 or −3 positions (Hennrich et al., 2013). We further examined whether any of these sites were phosphorylated in mitotic HeLa cells by a similar approach. As revealed by mass spectrometry, the VESS peptide containing both S64 and S65 was indeed found to be phosphorylated in vivo, but it was not possible to pinpoint which serine was phosphorylated (Figure 2, B and C). Because Mps1 prefers an acidic amino acid at −2 or −3 position for phosphorylation, we predicted S65 as the in vivo phosphorylation site, and attempted to develop phosphospecific antibodies against VESpS (S65). Unfortunately, this attempt was not successful. The antibody could not detect in vivo phosphorylation of
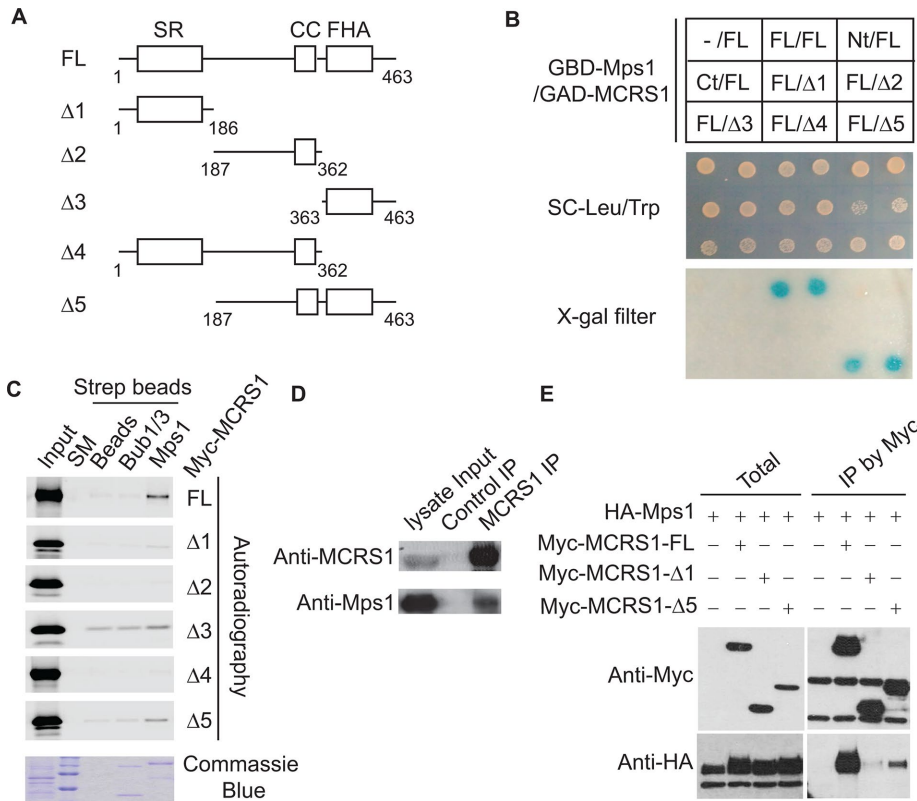
FIGURE 1: Mps1 interacts with MCRS1. (A) Functional domains and different truncations of MCRS1. SR, serine-rich domain; CC, coiled-coil domain; and FHA, forkhead-associated domain. (B) Yeast two-hybrid interaction of Mps1 and MCRS1. Mps1 fused to GAL4 DB and MCRS1 fused to GAL4 AD were expressed in yeast cells and β-galactosidase expression is monitored by X-gal filter assay. FL, full-length of proteins; Nt, N-terminal domain of Mps1; Ct, C-terminal domain of Mps1; and Δ1-5, different truncations of MCRS1. (C) In vitro binding assay of Mps1 and MCRS1. Strep-Mps1 was purified from SF9 cells and used as bait for binding of in vitro translated Myc-MCRS1 with S³⁵-methionine. Strep-Bub1Nt/Bub3 was used as a negative control for binding. SM, protein size marker. (D) CoIP experiment of endogenous Mps1 and MCRS1. HeLa Tet-on cells were arrested with nocodazole for 12 h. MCRS1 was pulled down by control or MCRS1 beads. Total lysates and IPed fractions were resolved by SDS–PAGE and processed for Western blot. (E) CoIP experiment of Mps1 and MCRS1. HA-Mps1 and Myc-MCRS1 were cotransfected into HeLa Tet-on cells and arrested at M-phase with nocodazole for 12 h. Myc-MCRS1 was pulled down by Myc beads. Total lysates and IPed fractions were resolved by SDS–PAGE and processed for Western blot.

depleted by RNA interference (RNAi) (Figure 3, A and B). The delayed chromosome alignment was likely the cause of the longer mitotic duration of the cells, as misaligned chromosomes were often observed in those cells (Supplemental Figure S1C). These cells eventually segregated their chromosomes after realigning chromosomes and exited mitosis. When cells were treated with taxol or nocodazole to examine the functionality of the SAC, most MCRS1-depleted cells arrested in mitosis, indicating that the SAC was not apparently compromised by MCRS1 depletion (Supplemental Figure S1, D and E). Inactivation of Mps1 has been shown to interrupt normal chromosome alignment in MG132-arrested metaphase cells (Hewitt et al., 2010; Santaguida et al., 2010; Dou et al., 2015). When we inactivated Mps1 with the small molecule inhibitor AZ3146 together with MG132, scattered chromosomes resulting from abnormal chromosome alignment were frequently observed in mitotic cells (see Figure 5, A and B, later in the paper). Thus, both MCRS1 and Mps1 are required for proper chromosome alignment in human cells, raising the possibility that their interaction or the phosphorylation of MCRS1 by Mps1 is functionally important for this process.

Phosphorylation of MCRS1 at S65 by Mps1 facilitates chromosome alignment

To test the function of MCRS1 S64/S65 phosphorylation in chromosome alignment, we developed HeLa cell lines stably expressing RNAi-resistant MCRS1 wild type or S64A/S65A (Supplemental Figure S2A). Reverse transcription-PCRs (RT-PCRs) and Western blots showed that the levels of endogenous MCRS1 mRNA and protein were greatly reduced by RNAi but those of exogenous MCRS1-GFP were not. MCRS1-GFP predominantly localized to the nucleus and nucleolus during interphase, but was enriched at the spindle poles, near the minus end of microtubules, from prophase to anaphase (Figure 3C). This is consistent with earlier findings that MCRS1 localizes to the minus end of microtubules during mitosis (Meunier and Vernos, 2011).

We then examined mitotic timing of the stable HeLa cell lines after MCRS1 RNAi (Supplemental Figure S2B). Many cells stayed in mitosis longer than 3 h and resulted in mitotic exit without division or mitotic cell death. Unlike control HeLa cells, HeLa cells stably expressing MCRS1-WT did not exhibit gross mitotic defect. By contrast, HeLa cells expressing MCRS1-S64A/S65A exhibited mitotic defect similar to control cells, and stayed longer in mitosis. To verify that the mitotic defect of MCRS1-S64A/S65A was not due to clonal variation, we generated additional clones of MCRS1 and examine their mitotic timing (Figure 3, D and E). We developed HeLa cell lines where MCRS1 expression was controllable by an inducible promoter to circumvent any potential harmful effect of MCRS1 overexpression during clonal development. Again, cells

MCRS1 in HeLa cells, possibly due to its low steady-state level or detection hindrance by neighboring phosphorylation at S64 or S69. However, the antibody could detect in vitro phosphorylation of wild-type MCRS1 protein after Mps1 kinase assay, but recognized the S65A mutant much less efficiently, indicating that S65 is an Mps1 site in vitro (Figure 2D). Although our data clearly show that S64/S65 is a phosphorylation site of MCRS1 in vitro and in vivo, we cannot ascertain whether Mps1 is the only kinase mediating this phosphorylation in vivo. Because the mitotic kinase Plk1 has a substrate specificity similar to that of Mps1, it is possible that Plk1 or other kinases can contribute to MCRS1 phosphorylation.

MCRS1 functions in chromosome alignment during mitosis

It was previously reported that MCRS1 facilitates metaphase chromosome alignment by regulating the minus-end kinetochore microtubule dynamics (Meunier and Vernos, 2011). Consistent with the earlier study, our time-lapse live-cell imaging showed that the mitotic duration of A549 cells was significantly extended when MCRS1 was
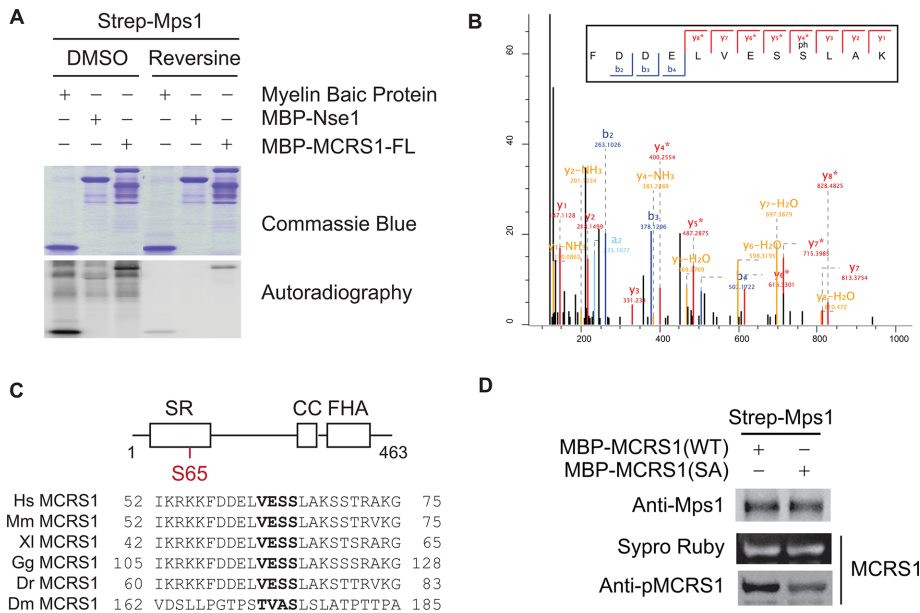
FIGURE 2: Mps1 phosphorylates MCRS1 at S64/S65 site. (A) In vitro Mps1 kinase assay. Strep-Mps1 was incubated with myelin basic protein, MBP-Nse1, or MBP-MCRS1 together with P^{32}-γ-ATP and its phosphorylation was monitored by autoradiography. (B) Mass profile of MCRS1 peptides containing phosphorylated S65. MCRS1-GFP-Strep was purified from HeLa cells and in vivo phosphorylation sites were analyzed by mass spectrometry. (C) Sequence homology of S65 region among metazoa MCRS1 orthologues. SR, serine rich; CC, coiled coiled; FHA, forkhead associated. (D) In vitro Mps1 kinase assay. Strep-Mps1 was incubated with MBP-MCRS1 wild-type or S64A/S65A proteins together with cold ATP, and its phosphorylation was monitored by anti-serum against pS65-MCRS1.

with the RNAi-resistant MCRS1-WT exited mitosis normally after MCRS1 RNAi, but cells with the MCRS1-S65A did not, ruling out clonal variation as the underlying cause of the observed mitotic phenotype. We also generated an inducible cell line of phosphorylation-mimicking MCRS1-S65D and examined its mitotic timing. This cell line behaved the same way as the wild-type cell line. The fact that the S65D mutant, but not the S65A mutant, can functionally complement MCRS1 depletion strongly supports the involvement of phosphorylation and argues against a simple structural role of S65.

To further study the defects of MCRS1-S65A in chromosome alignment, we examined chromosome distribution in MG132-arrested metaphase cells (Figure 3F and Supplemental Figure S2C). Consistent with the prolonged mitotic timing, the percentage of cells with misaligned chromosomes was greatly increased after MCRS1 RNAi. Expression of MCRS1-WT or S65D reduced the percentage of the misaligned cells, but expression of MCRS1-S65A did not. This result confirms the important role of MCRS1 phosphorylation for efficient chromosome alignment.

MCRS1 regulates microtubule dynamics at the minus end through KIF2A

We next explored how phosphorylation of S65 contributed to chromosome alignment. We first asked whether phosphorylation regulates the subcellular localization of MCRS1. Our immunofluorescence results showed that the MCRS1-S65A protein properly localized to the nucleus and nucleolus during interphase and to the vicinity of spindle poles during mitosis (Figure 4, A and B, and Supplemental Figure S2, D and E). Thus, MCRS1 phosphorylation does not play a major role in its localization.

We then turned our attention to the mitotic spindle structure because of earlier reports implicating MCRS1 in spindle organization (Meunier and Vernos, 2011; Meunier et al., 2016). Interestingly, we noticed that the two centrosomes in S65A-expressing cells depleted of endogenous MCRS1 were often farther separated from each other than those in wild-type–expressing cells (Figure 4A and Supplemental Figures S3A and S4A). Because MCRS1 is known to regulate microtubule dynamics at the minus end (Meunier and Vernos, 2011), this defect might be caused by deregulation of microtubule dynamics. Next, we measured the intercentrosome distance in metaphase cells arrested by MG132 (Figure 4, C and D, and Supplemental Figures S3B and S4A). In control cells, the intercentrosome distance was ~5–6 μm, but it was extended to ~8–9 μm after MCRS1 RNAi. Expression of MCRS1-WT or S65D reduced the distance to the control level, but expression of MCRS1-S65A did not. Therefore, phosphorylation of MCRS1 regulates the organization of the mitotic spindles at metaphase.

A recent study has shown that the MLL complex regulates intercentrosome distance through kinesin-13 family member, KIF2A (Ali et al., 2017). To test whether KIF2A was a downstream effector of MCRS1, we checked KIF2A localization in our stable cell lines. The level of KIF2A at the minus end of microtubules near the spindle poles was greatly reduced by MCRS1 depletion (Figure 4, C and E, and Supplemental Figures S3, C and D, and S4A), even though the total level of KIF2A protein was not altered (Figure 4F). Expression of MCRS1-WT or S65D restored KIF2A recruitment to the spindle poles, but expression of MCRS1-S65A did not. Consistently, we have detected a weak interaction between MCRS1 and KIF2A during mitosis (Figure 4F). KIF2A inactivation has been previously shown to result in chromosome segregation defects (Ganem and Compton, 2004; Rogers et al., 2004; Jang et al., 2009; Tanenbaum et al., 2009). Thus, we wondered whether depletion of KIF2A by small interfering RNA (siRNA) causes chromosome alignment defects. KIF2A was efficiently depleted by the siRNA (Figure 4F). Its depletion greatly increased cells with misaligned chromosomes (Supplemental Figure S5, A and B), further supporting KIF2A as a downstream effector of MCRS1 for chromosome alignment. We then tested whether the reduction of KIF2A by MCRS1 depletion is mediated by the delocalization of the MLL complex at the mitotic spindles. The localization of MLL1 at the mitotic spindle was not altered by MCRS1 depletion (Supplemental Figure S5, C and D), suggesting that MCRS1 does not control MLL localization.

Because Mps1 phosphorylates MCRS1 at S65 (Figure 2, B–D) and this phosphorylation regulates KIF2A localization to the minus end of the mitotic spindles (Figure 4E and Supplemental Figure S3D), we examined whether Mps1 inhibition alters KIF2A localization and intercentrosome distance. Inactivation of Mps1 by either the chemical inhibitor AZ3146 or RNAi reduced the level of KIF2A at the minus end of microtubules near spindle poles and resulted in an increased intercentrosome distance (Figure 5, A, C, and D, and
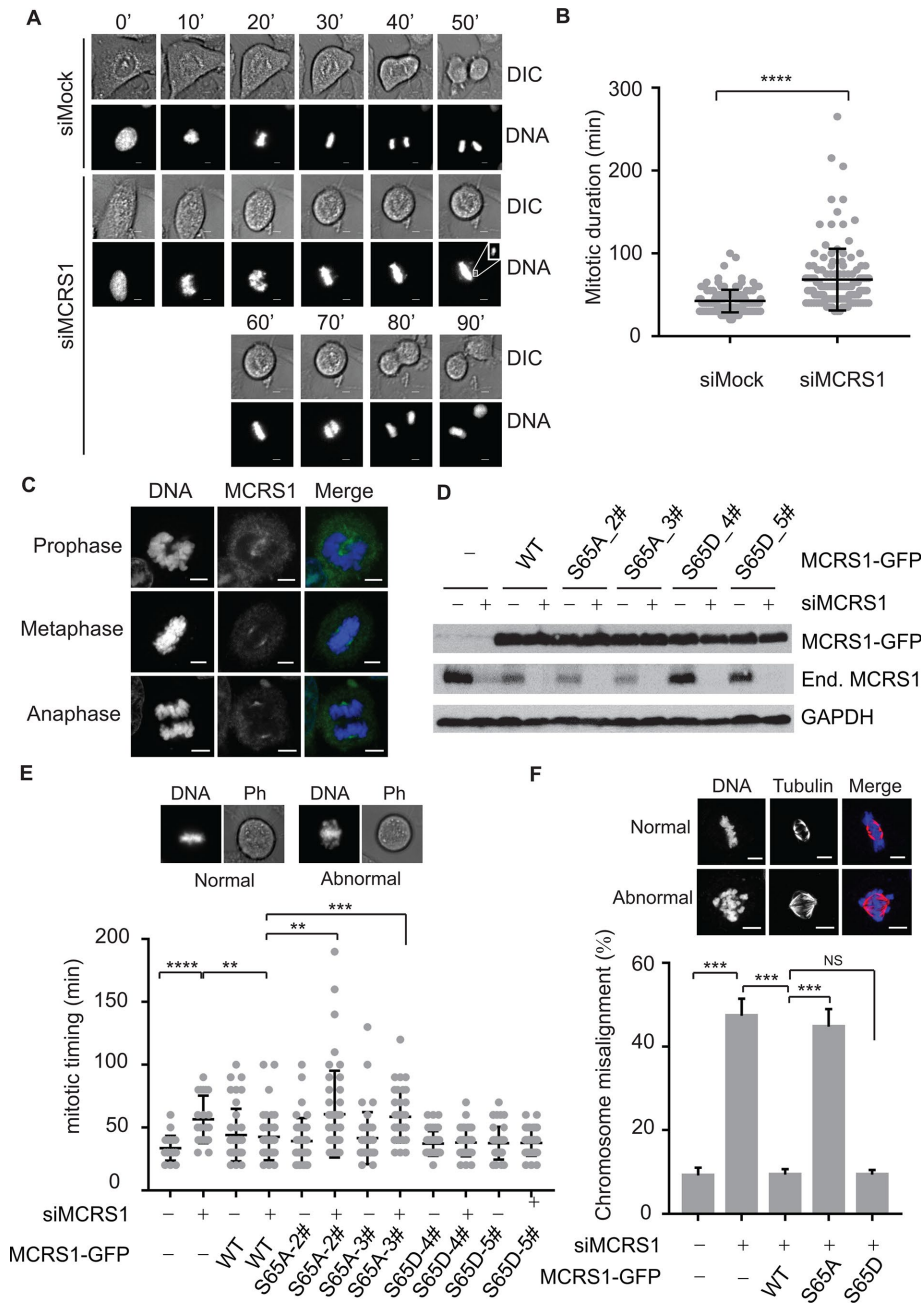
FIGURE 3: MCRS1 S65 phosphorylation-deficient mutant exhibits a defect in chromosome segregation. (A) Time-lapse live-cell images. A549 cells expressing H2B-CFP were transfected with MCRS1 siRNA. Cells were then arrested at G2 by RO3306 and released into fresh medium for monitoring chromosome segregation. Time after nuclear envelope breakdown was counted by minutes. Misaligned chromosomes in MCRS1 siRNA cells were magnified in a rectangle. Bar: 5 µm. (B) Mitotic duration of MCRS1 depleted cells. Results from three independent experiments of panel A were combined and are shown together as mean ± SEM (total 120 mitotic cells). Two-tailed P value was calculated by unpaired Student's t test. **** means P value is less than 0.0001, *** less than 0.001, and ** less than 0.01. NS stands for not significant. (C) Immunofluorescence of mitotic cells. HeLa Tet-on cells stably expressing MCRS1-GFP were fixed and processed for immunofluorescence using GFP antibody. DNA was stained by Hoechst 33342. Bar: 5 µm. (D) Stable cell line expressing MCRS1-GFP WT, S65A, or S65D. HeLa Tet-on cells were transfected with MCRS1 siRNA and processed for Western blot to examine MCRS1 protein level. (E) Mitotic duration of stable cell lines. Stable cell lines were transfected with siRNA and mitotic duration was counted by live-cell DIC microscope movie. Results from two independent experiments counting ~40 cells were combined and are shown here as mean ± SEM. Two-tailed P value was calculated similarly as in panel B. (F) Abnormal chromosome alignment at metaphase. Stable cell lines were transfected with siRNA and treated with MG132 for 1 h. Metaphase cells were counted either normal or abnormal, based on DNA and mitotic spindle distribution. Results from three independent experiments counting ~60 cells each were combined and are shown here as mean ± SEM. Two-tailed P value was calculated similarly as in panel B. Bar: 5 µm.

Supplemental Figure S6A). Next, we asked whether overexpression of MCRS1-S65D rescued chromosome alignment defect after Mps1 inhibition. Consistently, overexpression of MCRS1-WT or S65A did not rescue the alignment defect but that of MCRS1-S65D did (Figure 5E), strongly arguing that MCRS1 is a downstream target of Mps1 for chromosome alignment function. We also examined whether overexpression of KIF2A rescued the chromosome alignment defect of Mps1 inhibition or MCRS1 inactivation because KIF2A recruitment seems to be an important functional consequence of MCRS1 phosphorylation. Overexpression of KIF2A, however, did not rescue the alignment defect of Mps1 inhibition or MCRS1 inactivation, possibly due to the complex roles of KIF2A in chromosome segregation. Nonetheless, the level of centrosomal KIF2A was found to be anti-correlated to the intercentrosome distance, which further supports the role of KIF2A to regulate intercentrosome distance and chromosome alignment (Supplemental Figure S6B). Taken together, these results strongly suggest that MCRS1 phosphorylation by Mps1 regulates KIF2A localization and mitotic spindle dynamics to facilitate efficient chromosome alignment and proper segregation.

DISCUSSION

Mps1 is a potential molecular target of cancer chemotherapy, because of its myriad functions in mitosis (Salmela and Kallio, 2013; Dominguez-Brauer et al., 2015). In-depth studies of the SAC revealed detailed mechanisms by which Mps1 initiates the SAC signaling (Hiruma et al., 2015; Ji et al., 2015, 2017; Faesen et al., 2017). The molecular functions of Mps1 are not limited to the SAC, and include centrosome duplication, DNA damage repair, and chromosome alignment (Kasbek et al., 2007; Jelluma et al., 2008; Santaguida et al., 2010; Liu and Winey, 2012; Yu et al., 2016). Recent studies have shown that Mps1 plays an important regulatory role in chromosome alignment in metaphase by facilitating the localization of CENP-E, Aurora B, and Ska3 to kinetochores (Hewitt et al., 2010; van der Waal et al., 2012; Maciejowski et al., 2017). Our findings
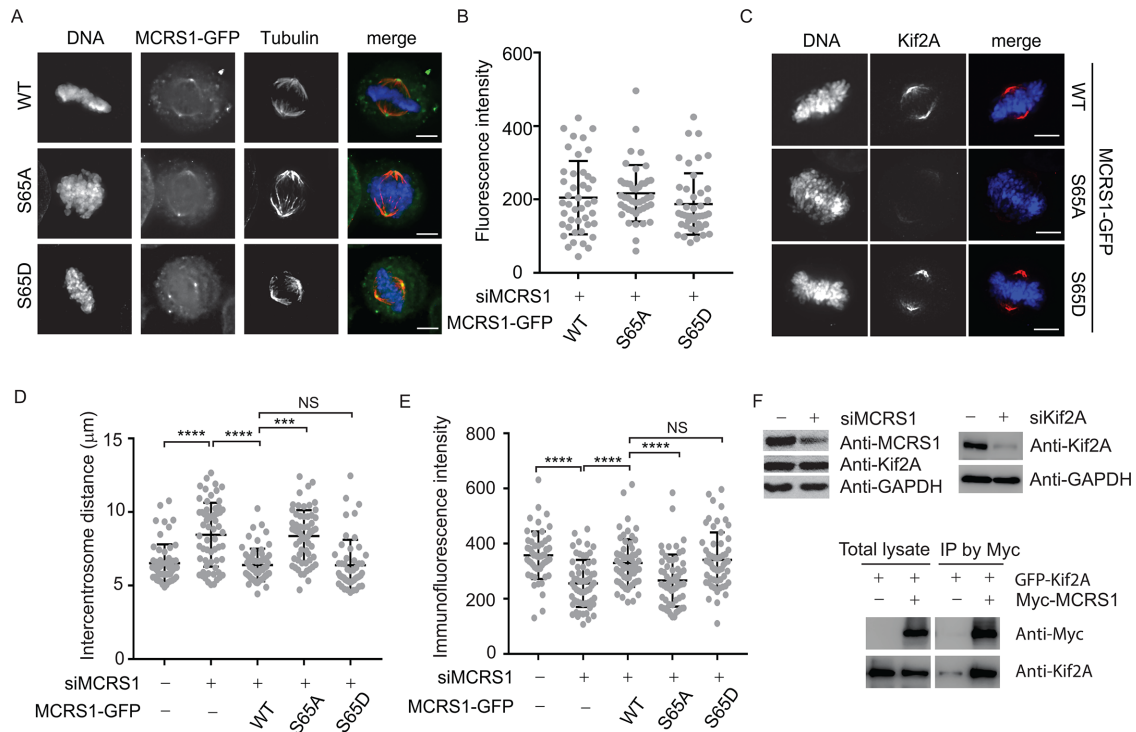
FIGURE 4: MCRS1 phosphorylation facilitates KIF2A recruitment to the spindle near centrosome.
(A) Immunofluorescence of stable cell lines. Stable cell lines were transfected with MCRS1 siRNA and treated with MG132 for 1 h. DNA, MCRS1-GFP, and mitotic spindle were visualized by Hoechst 33342, anti-GFP antibody, and anti-tubulin antibody. Bar: 5 μm. (B) Statistics of MCRS1-GFP intensity in stable cell line. The data from panel A were used for statistics. Results from two independent experiments counting ~40 cells were combined and are shown here as mean ± SEM. (C) Immunofluorescence of stable cell lines for KIF2A localization and intercentrosome distance. Stable cell lines were transfected with MCRS1 siRNA and treated with MG132 for 1 h. DNA and KIF2A were visualized by Hoechst 33342 and anti-KIF2A antibody. Bar: 5 μm. (D) Statistics of intercentrosome distance. The data from panel C were used for statistics. Results from two independent experiments counting ~60 cells were combined and are shown here as mean ± SEM. Two-tailed P value was calculated by unpaired Student's t test. **** means P value is less than 0.0001, *** less than 0.001, and NS means not significant. (E) Statistics of KIF2A localization in stable cell line. The data from panel D were used for statistics. Results from two independent experiments counting ~60 cells were combined and are shown here as mean ± SEM. Two-tailed P value was calculated similarly as in panel D. (F) Top panel, Kif2A level after siMCRS1 or siKif2A. HeLa Tet-on cells were subjected to MCRS RNAi or Kif2A RNAi and total lysates were resolved by SDS–PAGE and processed for Western blot. Bottom panel, CoIP experiment of MCRS1. Myc-MCRS1 and GFP-Kif2A were transfected into HeLa Tet-on cells and arrested at M-phase by nocodazole for 12 h. Myc-MCRS1 was pulled down by Myc beads. Total lysates and IPed fractions were resolved by SDS–PAGE and processed for Western blot with Myc or KIF2A antibody.

here further extend the functions of Mps1 to the regulation of microtubule minus-end dynamics at metaphase. Mps1 phosphorylates MCRS1 and targets it to spindle poles for proper regulation of the mitotic spindle. Mps1 and MCRS1 may act upstream of KIF2A, as Mps1 inhibition by AZ3146 reduces KIF2A localization and increases the length of the mitotic spindle.

It has been previously suggested that MCRS1 inhibits the recruitment of MCAK/KIF2C to the minus end of microtubules to prevent their inappropriate disassembly during early mitosis (Meunier and Vernos, 2011). Our study now reveals an active role of MCRS1 in recruiting KIF2A to the minus end of microtubules near the spindle poles. Our results seem to contradict the previous study, because KIF2A stimulates microtubule disassembly. KIF2A and KIF2C are members of the kinesin-13 family of microtubule motors, which facilitates the disassembly of microtubules. Although the two kinesins play similar roles in microtubule dynamics, they exhibit antagonistic effects on the assembly of the mitotic spindle and cell viability (Ganem and Compton, 2004; Rogers et al., 2004). Therefore, it is possible that MCRS1 may simultaneously inhibit MCAK and activate

KIF2A at the minus end of microtubules near the spindle poles. It is also possible that KIF2C may play a major role in determining the length of kinetochore microtubules, whereas KIF2A may primarily regulate the length of intercentrosome microtubules.

MCRS1 plays multiple roles during the cell cycle. It localizes to the nucleus and nucleolus to regulate gene expression as a member of the NSL complex in interphase and relocates to the minus end of kinetochore microtubules to regulate their dynamics (Lin and Shih, 2002; Okumura et al., 2005; Hirohashi et al., 2006; Andersen et al., 2010; Meunier and Vernos, 2011; Hsu et al., 2012; Fawal et al., 2015; Peng et al., 2015; Lee et al., 2016). The NSL complex is known to acetylate histone H4 to activate gene expression in interphase. Several members of this complex, including MCRS1, move to the minus ends of microtubules and regulate their dynamics (Meunier et al., 2015). It is noteworthy that the MLL complex, which mediates histone H3 methylation to activate gene expression, has also been shown to regulate mitotic spindle dynamics and share certain subunits with the NSL complex, including WDR5 and MCRS1 (Dou et al., 2005; Ali et al., 2017). Our study has now established an
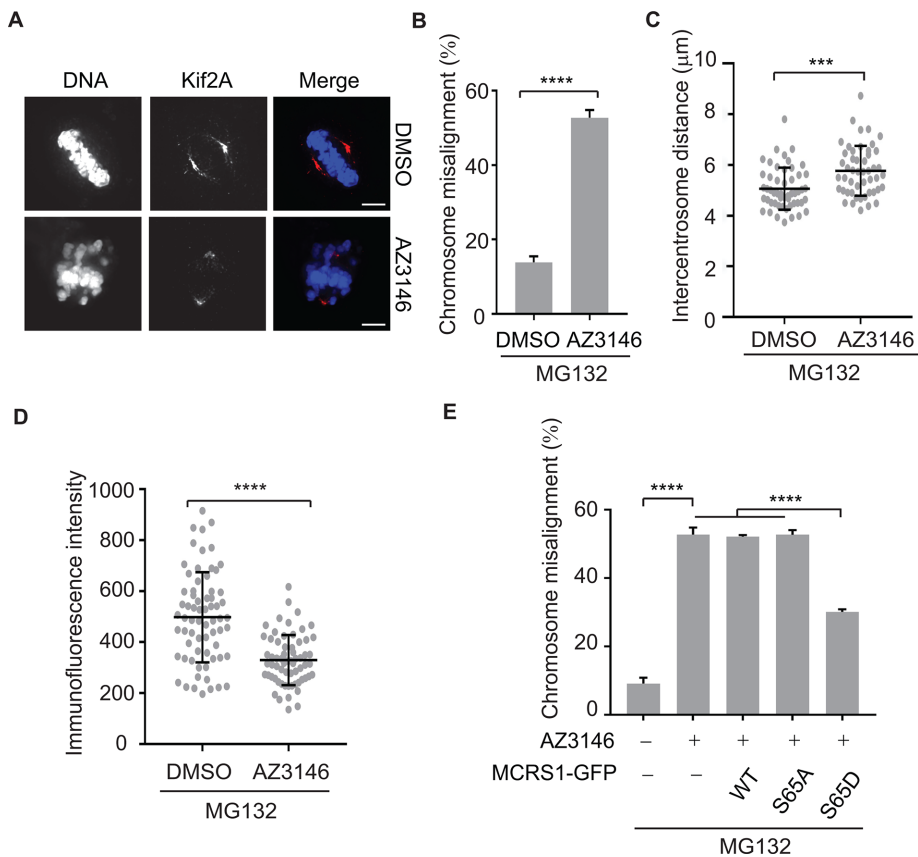
FIGURE 5: Mps1 inhibition diminishes KIF2A localization near centrosome. (A) Immunofluorescence of HeLa Tet-on cells after Mps1 inhibition. HeLa cells were treated with MG132 or MG132/AZ3146 for 1 h and processed for immunofluorescence to visualize DNA and KIF2A by Hoechst 33342 and anti-KIF2A antibody. Bar: 5 µm. (B) Statistics of abnormal chromosome alignment. The data from panel A were used for statistics and representative images of normal and abnormal alignment were shown in panel A. Results from three independent experiments counting ~100 cells each were combined and are shown here as mean ± SEM. Two-tailed P value was calculated by unpaired Student's t test. **** means P value is less than 0.0001 and *** less than 0.001. (C, D) Statistics of KIF2A localization and intercentrosome distance. The data from panel A were used statistics. Results from two independent experiments counting ~50 cells were combined and are shown here as mean ± SEM. Two-tailed P value was calculated similarly as in panel B. (E) Rescue of chromosome alignment defect. HeLa Tet-on cells expressing RNAi-resistant MCRS1-GFP were first transfected with MCRS1 siRNA and treated with MG132/AZ3146 for 1 h. Results from three independent experiments counting ~100 cells each were combined and are shown here as mean ± SEM. Two-tailed P value was calculated similarly as in panel B.

important Mps1-dependent regulatory mechanism that promotes MCRS1 function during mitosis.

MCRS1 is often overexpressed in multiple tumors, and its overexpression facilitates anchorage-independent growth and metastasis in those tumors (Bader *et al.*, 2001; Liu *et al.*, 2014). It will be interesting to test whether the mitotic function of MCRS1 and its regulation by Mps1 described herein are defective during tumorigenesis and whether these defects can be exploited for cancer therapy.

MATERIALS AND METHODS
Cell culture and transfection
HeLa Tet-on cells (Clontech) and A549 (American Type Culture Collection) cells were grown at 37°C in DMEM (Life Technologies) supplemented with 10% fetal bovine serum (Life Technologies) in a humid atmosphere with 5% CO_2. For mitotic arrest, cells were treated with 330 nM nocodazole (Sigma) or 100 nM taxol (Sigma) for

12–14 h. For chromosome alignment assay, 10 µM MG132 was treated for 1–2 h. For the generation of stable cell lines, HeLa Tet-On cells were transfected with pIRES-puro or pTRE2-hyg vectors encoding siRNA-resistant wild-type or mutant MCRS1-GFP transgenes. Clones of cells were selected in regular media containing 1 µg/ml puromycin (Mesgen) or 200–400 µg/ml hygromycin (Mesgen) and maintained in media with 0.8 µg/ml puromycin or 100 µg/ml hygromycin. Doxycycline (5 µg/ml; Mesgen) was used for induction of MCRS1 expression. For RNAi experiment, cells were transfected with siRNA oligonucleotides (Genepharma) using Lipofectamine RNAiMAX (Invitrogen) for 24–48 h. The sequences of the MCRS1 siRNAs were 5′-gcgugugaagaagaguaaa-3′. Plasmid transfection was carried out by Effectene reagent (Qiagen) according to the manufacturer's instructions.

Yeast two hybrid
The yeast two-hybrid screen was performed with the full-length Mps1 cloned in frame with the GAL4 DNA-binding domain of vector pGBKT7 (Clontech). The yeast cells were transformed with pGBKT7-Mps1 and the human Jurkat cDNA library (a gift of Michael White, Department of Cell Biology, University of Texas Southwestern Medical Center, Dallas, TX) and screened by growth in selective media. The positive clones were subsequently retested in fresh yeast cells, and the identities of preys were determined by DNA sequencing.

In vitro kinase assay
For IP-kinase assays, Strep-Mps1 was immunoprecipitated by Strep-Tactin Superflow resin (IBA Lifescience) in lysis buffer (25 mM Tris, pH 8.0, 150 mM KCl, 1 mM dithiothreitol [DTT], 0.2% NP-40, 5% glycerol, 0.1 mM phenylmethylsulfonyl fluoride, protease inhibitor cocktail [Sigma], and phosphatase inhibitor cocktail [Mesgen]) from SF9 cells and the Strep IPs were incubated with substrates in kinase buffer (25 mM Tris, pH 8.0, 0.15 M KCl, 10 mM $MgCl_2$, 1 mM DTT, 10 mM NaF, 5 mM β-glycerophosphate, 5% glycerol) containing 0.2 mM ATP and 0.1 µCi/µl γ-[^{32}P]ATP for 1 h at room temperature (RT) with vortex. The reaction mixture was quenched with SDS sample buffer, separated on SDS–PAGE, and analyzed by autoradiography. For inhibition of Mps1, 10 µM of reversine (Sigma) was added in the kinase reactions.

Direct binding assay
For protein-binding assays, purified Strep-Mps1 or Strep-Bub1-Nt/Bub3 were immobilized on Strep-tactin beads in binding buffer (25 mM Tris, pH 8.0, 0.15 M KCl, 0.2% NP-40, 5% glycerol, 1 mM DTT) containing 5% nonfat dry milk. After being washed twice, the beads were incubated with MCRS1 proteins translated in vitro by rabbit reticulocyte lysate (Promega) containing 0.5 µCi/µl [^{35}S]methionine

for 1 h at RT. After being washed two times, bound proteins were eluted with SDS sample buffer and analyzed by SDS–PAGE followed by autoradiography.

Antibodies and immunoprecipitation
The following primary antibodies were used for immunofluorescence: anti–β-tubulin (CWBIO; 1:500), anti-GFP (Proteintech, 1:300), and anti-KIF2A (Proteintech; 1:300). The following primary antibodies were used for Western blot: anti-Myc (Proteintech; 1:1000), anti-HA (Roche; 1:1000), anti-GAPDH (Mesgen; 1:5000), anti-actin, anti-Mps1, anti-H3pS10 (Cell Signaling; 1:1000), and anti-MCRS1 (Proteintech; 1:2000). The following secondary antibodies were used for immunofluorescence and Western blot: goat anti-mouse immunoglobulin G (IgG), horseradish peroxidase (HRP) conjugate (Proteintech; 1:5000), goat anti-rabbit IgG, HRP conjugate (Proteintech; 1:5000), goat–anti-rabbit IgG, FITC conjugated (CWBIO; 1:300), goat–anti-rabbit IgG, TRIRC conjugated (CWBIO; 1:300), goat–anti-mouse IgG, FITC conjugated (CWBIO; 1:300), and goat–anti-mouse IgG, TRITC conjugated (CWBIO; 1:300). Anti–pS65-MCRS1 antibody was generated by immunizing rabbits with the following peptide: ELVES-pS-LAKSSCys.

Mitotic cells coexpressing HA-Mps1 and Myc-MCRS1 were incubated with lysis buffer (25 mM Tris-HCl, pH 7.4, 150 mM NaCl, 1% NP-40, 1 mM EDTA, 5% glycerol) supplemented with protease inhibitor cocktail (Sigma) and phosphatase inhibitor cocktail (Mesgen) on ice for 5 min before scraping and cell lysates were cleared by centrifugation. The supernatants were incubated with anti–c-Myc magnetic beads (Pierce) at RT for 30 min and proteins bound to beads were released with SDS loading buffer, resolved in SDS–PAGE, and analyzed by Western blotting.

Immunofluorescence and imaging
Cells grown on coverslips were preextracted in PHEM buffer (60 mM PIPES, 25 mM HEPES, 10 mM EGTA [ethylene glycol tetraacetic acid], 4 mM MgSO$_4$, pH 7.0) containing 0.05% digitonin for 5 min and fixed by 4% paraformaldehyde in PBS at RT for 10 min. Cells were then permeabilized with PBST (phosphate-buffered saline containing 0.1% Triton X-100) and blocked with PBST containing 3% bovine serum albumin for 30 min. Primary antibodies were incubated at RT for 2 h and secondary antibodies for 1 h. DNA was stained by Hoechest 33342 (1 μg/ml) for 1 min. Cell images were acquired either by a 20× objective lens in a Nikon Eclipse Ti-E microscope for statistics and by a 60× objective lens in a Zeiss confocal microscope or a 100× objective lens in a Nikon Eclipse Ti-E microscope for representative images. The average of total protein intensity in small areas of two centrosomes subtracted by similar areas of mitotic cytoplasm in the same cell was used for quantification statistics. Law images from Nikon microscope were deconvoluted by NIS-element (Nikon) software and processed with ImageJ and Photoshop (Adobe). Fluorescence time-lapse imaging of A549 cells expressing CFP-H2B was recorded every 10 min for a total duration of 24 h with a 10× objective in a Nikon Eclipse Ti-E microscope equipped with a temperature- and CO$_2$-controlled stage incubation unit (Okolab).

Mass spectrometry analysis
MCRS1 proteins were purified from HeLa Tet-on cells stably expressing MCRS1-GFP-Strep by Strep-Tactin beads (IBA Lifescience) and digested by LysC enzyme (Promega). Peptides were separated and analyzed on an Easy-nLC 1000 system coupled to a Q Exactive HF (both from Thermo Scientific). About 2 μg of peptides was separated in a homemade column (75 μm × 15 cm) packed with C18 AQ

(5 μm, 300Å; Michrom BioResources) at a flow rate of 300 nl/min. Mobile phase A (0.1% formic acid in 2% ACN [acetonitrile]) and mobile phase B (0.1% formic acid in 98% ACN) were used to establish a 60-min gradient composed of 2 min of 5% B, 40 min of 5–30% B, 6 min of 30–45% B, 2 min of 45–90% B, and 10 min of 90% B. Peptides were then ionized by electrospray at 2.3 kV. A full MS spectrum (300–1800 m/z range) was acquired at a resolution of 120,000 at m/z 200 and a maximum ion accumulation time of 20 ms. Dynamic exclusion was set to 30 s. Resolution for HCD MS/MS spectra was set to 30,000 at m/z 200. The AGC setting of MS and MS^2 were set at 3E6 and 1E5, respectively. The 20 most intense ions above a 1.3E4-count threshold were selected for fragmentation by HCD with a maximum ion accumulation time of 80 ms. Isolation width of 1.6 m/z units was used for MS^2. Single and unassigned charged ions were excluded from MS/MS. For HCD, normalized collision energy was set to 30%. The underfill ratio was defined as 1%.

The raw data were processed and searched with MaxQuant 1.5.4.1 with MS tolerance of 4.5 ppm, and MS/MS tolerance of 20 ppm. The MCRS1 protein sequence and database for proteomics contaminants from MaxQuant were used for database searches. Reversed database searches were used to evaluate the false discovery rate (FDR) of peptide and protein identifications. Two missed cleavage sites of Lys-C were allowed. Oxidation (M), acetyl (protein N-term), deamidation (NQ), and phosphorylation (STY) were set as variable modifications. The FDR of both peptide identification and protein identification is set to be 1%. The option of "Second peptides," "Match between runs," and "Dependent peptides" was enabled.

REFERENCES
Ali A, Veeranki SN, Chinchole A, Tyagi S (2017). MLL/WDR5 complex regulates Kif2A localization to ensure chromosome congression and proper spindle assembly during mitosis. Dev Cell 41, 605–622 e607.

Andersen DS, Raja SJ, Colombani J, Shaw RL, Langton PF, Akhtar A, Tapon N (2010). *Drosophila* MCRS2 associates with RNA polymerase II complexes to regulate transcription. Mol Cell Biol 30, 4744–4755.

Bader AG, Schneider ML, Bister K, Hartl M (2001). TOJ3, a target of the v-Jun transcription factor, encodes a protein with transforming activity related to human microspherule protein 1 (MCRS1). Oncogene 20, 7524–7535.

Cavazza T, Vernos I (2015). The RanGTP pathway: from nucleo-cytoplasmic transport to spindle assembly and beyond. Front Cell Dev Biol 3, 82.

Dominguez-Brauer C, Thu KL, Mason JM, Blaser H, Bray MR, Mak TW (2015). Targeting mitosis in cancer: emerging strategies. Mol Cell 60, 524–536.

Dou Z, Liu X, Wang W, Zhu T, Wang X, Xu L, Abrieu A, Fu C, Hill DL, Yao X (2015). Dynamic localization of Mps1 kinase to kinetochores is essential for accurate spindle microtubule attachment. Proc Natl Acad Sci USA 112, E4546–E4555.

Dou Y, Milne TA, Tackett AJ, Smith ER, Fukuda A, Wysocka J, Allis CD, Chait BT, Hess JL, Roeder RG (2005). Physical association and coordinate function of the H3 K4 methyltransferase MLL1 and the H4 K16 acetyltransferase MOF. Cell 121, 873–885.

Espeut J, Gaussen A, Bieling P, Morin V, Prieto S, Fesquet D, Surrey T, Abrieu A (2008). Phosphorylation relieves autoinhibition of the kinetochore motor Cenp-E. Mol Cell 29, 637–643.

Faesen AC, Thanasoula M, Maffini S, Breit C, Muller F, van Gerwen S, Bange T, Musacchio A (2017). Basis of catalytic assembly of the mitotic checkpoint complex. Nature 542, 498–502.

Fawal MA, Brandt M, Djouder N (2015). MCRS1 binds and couples Rheb to amino acid-dependent mTORC1 activation. Dev Cell 33, 67–81.

Ganem NJ, Compton DA (2004). The KinI kinesin Kif2a is required for bipolar spindle assembly through a functional relationship with MCAK. J Cell Biol 166, 473–478.

Godek KM, Kabeche L, Compton DA (2015). Regulation of kinetochore-microtubule attachments through homeostatic control during mitosis. Nat Rev Mol Cell Biol 16, 57–64.

Hennrich ML, Marino F, Groenewold V, Kops GJ, Mohammed S, Heck AJ (2013). Universal quantitative kinase assay based on diagonal SCX chromatography and stable isotope dimethyl labeling provides high-definition kinase consensus motifs for PKA and human Mps1. J Proteome Res 12, 2214–2224.

Hewitt L, Tighe A, Santaguida S, White AM, Jones CD, Musacchio A, Green S, Taylor SS (2010). Sustained Mps1 activity is required in mitosis to recruit O-Mad2 to the Mad1-C-Mad2 core complex. J Cell Biol 190, 25–34.

Hirohashi Y, Wang Q, Liu Q, Du X, Zhang H, Sato N, Greene MI (2006). p78/MCRS1 forms a complex with centrosomal protein Nde1 and is essential for cell viability. Oncogene 25, 4937–4946.

Hiruma Y, Sacristan C, Pachis ST, Adamopoulos A, Kuijt T, Ubbink M, von Castelmur E, Perrakis A, Kops GJ (2015). Competition between MPS1 and microtubules at kinetochores regulates spindle checkpoint signaling. Science 348, 1264–1267.

Hsu CC, Lee YC, Yeh SH, Chen CH, Wu CC, Wang TY, Chen YN, Hung LY, Liu YW, Chen HK, et al. (2012). 58-kDa microsphenule protein (MSP58) is novel Brahma-related gene 1 (BRG1)-associated protein that modulates p53/p21 senescence pathway. J Biol Chem 287, 22533–22548.

Ivanova AV, Ivanov SV, Lerman ML (2005). Association, mutual stabilization, and transcriptional activity of the STRA13 and MSP58 proteins. Cell Mol Life Sci 62, 471–484.

Jang CY, Coppinger JA, Seki A, Yates JR, 3rd, Fang G (2009). Plk1 and Aurora A regulate the depolymerase activity and the cellular localization of Kif2a. J Cell Sci 122, 1334–1341.

Jelluma N, Brenkman AB, van den Broek NJ, Cruijsen CW, van Osch MH, Lens SM, Medema RH, Kops GJ (2008). Mps1 phosphorylates Borealin to control Aurora B activity and chromosome alignment. Cell 132, 233–246.

Ji Z, Gao H, Jia L, Li B, Yu H (2017). A sequential multi-target Mps1 phosphorylation cascade promotes spindle checkpoint signaling. Elife 6, e22513.

Ji Z, Gao H, Yu H (2015). Kinetochore attachment sensed by competitive Mps1 and microtubule binding to Ndc80C. Science 348, 1260–1264.

Kasbek C, Yang CH, Yusof AM, Chapman HM, Winey M, Fisk HA (2007). Preventing the degradation of mps1 at centrosomes is sufficient to cause centrosome reduplication in human cells. Mol Biol Cell 18, 4457–4469.

Lan W, Cleveland DW (2010). A chemical tool box defines mitotic and interphase roles for Mps1 kinase. J Cell Biol 190, 21–24.

Lee SH, Lee MS, Choi TI, Hong H, Seo JY, Kim CH, and Kim J (2016). MCRS1 associates with cytoplasmic dynein and mediates pericentrosomal material recruitment. Sci Rep 6, 27284.

Lin DY, Shih HM (2002). Essential role of the 58-kDa microsphenule protein in the modulation of Daxx-dependent transcriptional repression as revealed by nucleolar sequestration. J Biol Chem 277, 25446–25456.

Liu X, Winey M (2012). The MPS1 family of protein kinases. Annu Rev Biochem 81, 561–585.

Liu MX, Zhou KC, Cao Y (2014). MCRS1 overexpression, which is specifically inhibited by miR-129*, promotes the epithelial-mesenchymal transition and metastasis in non-small cell lung cancer. Mol Cancer 13, 245.

London N, Biggins S (2014). Mad1 kinetochore recruitment by Mps1-mediated phosphorylation of Bub1 signals the spindle checkpoint. Genes Dev 28, 140–152.

London N, Ceto S, Ranish JA, Biggins S (2012). Phosphoregulation of Spc105 by Mps1 and PP1 regulates Bub1 localization to kinetochores. Curr Biol 22, 900–906.

Maciejowski J, Drechsler H, Grundner-Culemann K, Ballister ER, Rodriguez-Rodriguez JA, Rodriguez-Bravo V, Jones MJK, Foley E, Lampson MA, Daub H, et al. (2017). Mps1 regulates kinetochore-microtubule attachment stability via the Ska complex to ensure error-free chromosome segregation. Dev Cell 41, 143–156 e146.

Manning AL, Ganem NJ, Bakhoum SF, Wagenbach M, Wordeman L, Compton DA (2007). The kinesin-13 proteins Kif2a, Kif2b, and Kif2c/MCAK have distinct roles during mitosis in human cells. Mol Biol Cell 18, 2970–2979.

Meunier S, Shvedunova M, Van Nguyen N, Avila L, Vernos I, Akhtar A (2015). An epigenetic regulator emerges as microtubule minus-end binding and stabilizing factor in mitosis. Nat Commun 6, 7889.

Meunier S, Timon K, Vernos I (2016). Aurora-A regulates MCRS1 function during mitosis. Cell Cycle 15, 1779–1786.

Meunier S, Vernos I (2011). K-fibre minus ends are stabilized by a RanGTP-dependent mechanism essential for functional spindle assembly. Nat Cell Biol 13, 1406–1414.

Mora-Santos MD, Hervas-Aguilar A, Sewart K, Lancaster TC, Meadows JC, Millar JB (2016). Bub3-Bub1 binding to Spc7/KNL1 toggles the spindle checkpoint switch by licensing the interaction of Bub1 with Mad1-Mad2. Curr Biol 26, 2642–2650.

Musacchio A (2015). The molecular biology of spindle assembly checkpoint signaling dynamics. Curr Biol 25, R1002–R1018.

Okumura K, Zhao M, Depinho RA, Furnari FB, Cavenee WK (2005). Cellular transformation by the MSP58 oncogene is inhibited by its physical interaction with the PTEN tumor suppressor. Proc Natl Acad Sci USA 102, 2703–2706.

Peng J, Ma J, Li W, Mo R, Zhang P, Gao K, Jin X, Xiao J, Wang C, Fan J (2015). Stabilization of MCRS1 by BAP1 prevents chromosome instability in renal cell carcinoma. Cancer Lett 369, 167–174.

Ren Y, Busch RK, Perlaky L, Busch H (1998). The 58-kDa microsphenule protein (MSP58), a nucleolar protein, interacts with nucleolar protein p120. Eur J Biochem 253, 734–742.

Rogers GC, Rogers SL, Schwimmer TA, Ems-McClung SC, Walczak CE, Vale RD, Scholey JM, Sharp DJ (2004). Two mitotic kinesins cooperate to drive sister chromatid separation during anaphase. Nature 427, 364–370.

Sacristan C, Kops GJ (2014). Joined at the hip: kinetochores, microtubules, and spindle assembly checkpoint signaling. Trends Cell Biol 25, 21–28.

Salmela AL, Kallio MJ (2013). Mitosis as an anti-cancer drug target. Chromosoma 122, 431–449.

Santaguida S, Tighe A, D'Alise AM, Taylor SS, Musacchio A (2010). Dissecting the role of MPS1 in chromosome biorientation and the spindle checkpoint through the small molecule inhibitor reversine. J Cell Biol 190, 73–87.

Shepperd LA, Meadows JC, Sochaj AM, Lancaster TC, Zou J, Buttrick GJ, Rappsilber J, Hardwick KG, Millar JB (2012). Phosphodependent recruitment of Bub1 and Bub3 to Spc7/KNL1 by Mph1 kinase maintains the spindle checkpoint. Curr Biol 22, 891–899.

Tanenbaum ME, Macurek L, Janssen A, Geers EF, Alvarez-Fernandez M, Medema RH (2009). Kif15 cooperates with eg5 to promote bipolar spindle assembly. Curr Biol 19, 1703–1711.

Uehara R, Tsukada Y, Kamasaki T, Poser I, Yoda K, Gerlich DW, Goshima G (2013). Aurora B and Kif2A control microtubule length for assembly of a functional central spindle during anaphase. J Cell Biol 202, 623–636.

van der Waal MS, Saurin AT, Vromans MJ, Vleugel M, Wurzenberger C, Gerlich DW, Medema RH, Kops GJ, Lens SM (2012). Mps1 promotes rapid centromere accumulation of Aurora B. EMBO Rep 13, 847–854.

Welburn JP, Cheeseman IM (2012). The microtubule-binding protein Cep170 promotes the targeting of the kinesin-13 depolymerase Kif2b to the mitotic spindle. Mol Biol Cell 23, 4786–4795.

Wu JL, Lin YS, Yang CC, Lin YJ, Wu SF, Lin YT, Huang CF (2009). MCRS2 represses the transactivation activities of Nrf1. BMC Cell Biol 10, 9.

Yamagishi Y, Yang CH, Tanno Y, Watanabe Y (2012). MPS1/Mph1 phosphorylates the kinetochore protein KNL1/Spc7 to recruit SAC components. Nat Cell Biol 14, 746–752.

Yang CP, Chiang CW, Chen CH, Lee YC, Wu MH, Tsou YH, Yang YS, Chang WC, Lin DY (2015). Identification and characterization of nuclear and nucleolar localization signals in 58-kDa microsphenule protein (MSP58). J Biomed Sci 22, 33.

Yu ZC, Huang YF, Shieh SY (2016). Requirement for human Mps1/TTK in oxidative DNA damage repair and cell survival through MDM2 phosphorylation. Nucleic Acids Res 44, 1133–1150.